An Atomization Model for Splash Plate Nozzles

Araz Sarchami and Nasser Ashgriz
Mechanical and Engineering Dept., University of Toronto, Toronto, Ontario, M5S 3G8 Canada

Honghi Tran
Chemical Engineering Dept., Pulp and Paper Center, University of Toronto, Toronto, Ontario, M5S 3E5 Canada

DOI 10.1002/aic.12033
Published online September 29, 2009 in Wiley InterScience (www.interscience.wiley.com).

A model for the atomization and spray formation by splash plate nozzles is presented. This model is based on the liquid sheet formation theory due to an oblique impingement of a liquid jet on a solid surface. The continuous liquid sheet formed by the jet impingement is replaced with a set of dispersed droplets. The initial droplet sizes and velocities are determined based on theoretically predicted liquid sheet thickness and velocity. A Lagrangian spray code is used to model the spray dynamics and droplet size distribution further downstream of the nozzle. Results of this model are confirmed by the experimental data on the droplet size distribution across the spray. © 2009 American Institute of Chemical Engineers *AIChE J,* 56: 849–857, 2010
Keywords: splash plate nozzle, atomization, recovery boiler, numerical simulation, droplet size

Introduction

Liquid sheet (or film) atomizers are widely used in gas turbines, automobiles, and liquid-fueled rocket engines. They are also the most commonly used nozzles in Kraft recovery boilers to spray black liquor, a byproduct of paper making, into a furnace. One type of liquid sheet atomizers is jet impinging nozzles (i.e., splash plate nozzles)[1,2]. In such nozzles, a liquid jet impinges on a splash plate and spreads out radially while thinning. The thinning liquid sheet later breaks into small droplets forming the spray. This method has several advantages, such as low injection pressure loss and high controllability of liquid sheet thickness, velocity, trajectory, and mass distribution.[3] Prediction of droplet size and velocity distribution produced by these nozzles is needed for engine design and for the improvement of combustion processes. Such predictions require information on the liquid sheet characteristics and its breakup process.

Taylor[4] and Dombrowski et al.[5] have conducted extensive studies on the liquid sheet characteristics. Taylor[4] proposed a model for the variation of the thickness of the liquid sheet, by neglecting the surface tension and viscosity, and assuming a constant velocity throughout the sheet. Dombrowski et al.[5] developed a model for the sheet formation based on an assumption that the thickness of the sheet, at any point, is inversely proportional to its distance from the orifice.

Once the liquid sheet is formed, it becomes unstable and breaks into small droplets. The problem of sheet instability is extensively studied, starting with the experiments of Savart.[6] Dorman[7] and Fraser and Eisenklam[8] and later Dombrowski and Fraser[9] provided the early quantitative analysis of the problem. Three modes of disintegrations were identified and were referred to as the rim breakup, wave instability, and sheet perforation.[8,9] All three modes of breakups may occur in jet impinging atomizers and most of the time a combination of these regimes causes the breakup while one of them is the dominant regime. Numerical studies on the entire process of sheet formation and breakup and consequent droplet size distribution are very limited. Levesque and coworkers[10] simulated flow injection, sheet formation, and breakup from a jet impinging nozzle. They developed a three dimensional code, which predicted liquid free-surface evolution and breakups. Their model does not consider effects of surrounding gases on the sheet breakup. Foust et al.[10] using a three dimensional volume of fluid method simulated a scaled splash plate nozzles and studied spray characteristics using black liquor as injection fluid.

Correspondence concerning this article should be addressed to N. Ashgriz at ashgriz@mie.utoronto.ca

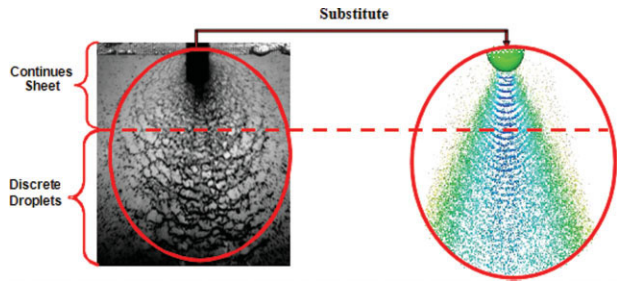

Figure 1. Analogy between continuous sheet and discrete droplets.

[Color figure can be viewed in the online issue, which is available at www.interscience.wiley.com.]

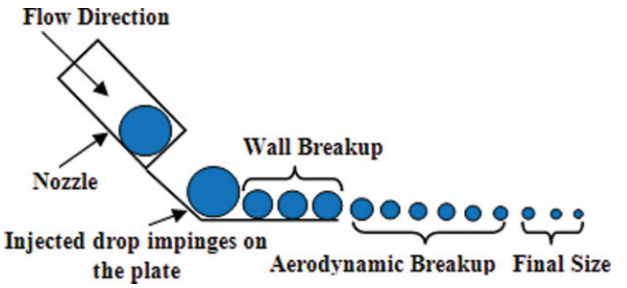

Figure 3. Side view of droplets impinging on the splash plate.

[Color figure can be viewed in the online issue, which is available at www.interscience.wiley.com.]

To predict the size of the droplets that form from jet impinging nozzles, we first need to characterize the liquid sheet, namely its velocity and thickness distribution. Such information is obtained from a model by Inamura et al.[3] Data from this model are incorporated into a Lagrangian spray code to predict droplet size and velocity distribution downstream of the flow.

Methodology

General procedure

In a wall impingement nozzle, a continuous liquid jet impinges on a surface (i.e., the splash plate) and spreads out radially forming a liquid sheet. Later, this liquid sheet breaks into small droplets forming the spray. Here, instead of a continuous liquid jet, streams of droplets are made to impinge onto the plate, which spread out radially and later breakup to form the spray. The final outcome of the two processes (continuous jet and discrete droplet impingement) can be the same if a proper model is used for the breakup of the droplets after impingement (e.g., a splash plate model). Figure 1 shows the schematic of proposed analogy between continuous sheet and discrete droplet spray.

The goal here is to develop a numerical procedure to predict the final droplet size and velocity distributions downstream of the spray based on the thickness and velocity distributions of the liquid sheet formed after impingement on the splash plate. To achieve this, the procedure begins with droplet injection right from the nozzle with the diameter equal to the splash plate nozzle diameter. The injected droplets hit the splash plate and break into several smaller droplets. Figure 2 shows top view of the splash plate atomizer at the time of injection. The smaller droplets are distributed azimuthally on the plate. Each droplet at any specific trajectory has a specific velocity and size, equal to the sheet thickness and velocity at that trajectory (i.e., azimuthall angle). The model intends to substitute the smooth fluid sheet on the plate with discretized droplets having the same diameter (thickness) and velocity as the sheet.

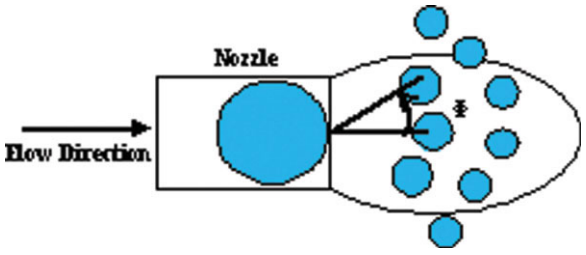

Figure 2. Top view of droplets injected from a nozzle.

[Color figure can be viewed in the online issue, which is available at www.interscience.wiley.com.]

Figure 3 shows side view of the droplet impingement. While droplets move further downstream, they interact with the surrounding gas and each other. Droplets will break, coalesce, disperse, and evaporate. Figure 4 demonstrates the process from the injection at the nozzle to the final droplet size results.

An analytical model by Inamura et al.[3] is used to describe the sheet thickness and velocity distribution on the plate. They have developed a model for the oblique impingement of a jet on a solid wall. They have considered a two dimensional laminar boundary layer flow with uniform jet velocity. Figures 5a, b show schematics of the jet impingement and sheet formation, describing important governing parameters.

Splash plate model

Inamura et al.[3] found the sheet thickness and velocity distribution by solving continuity and momentum equations inside the boundary layer. The momentum equation of a

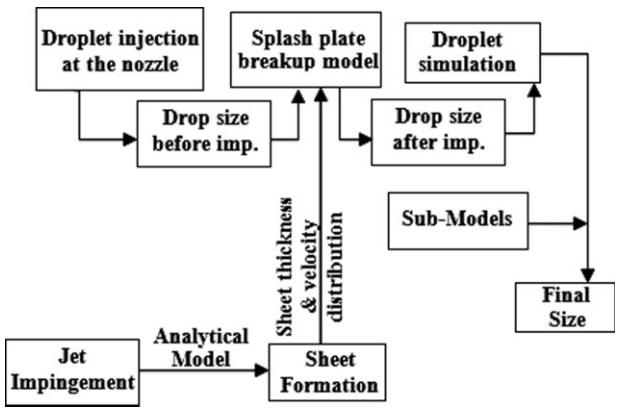

Figure 4. Process flowchart for the splash plate nozzle simulation.

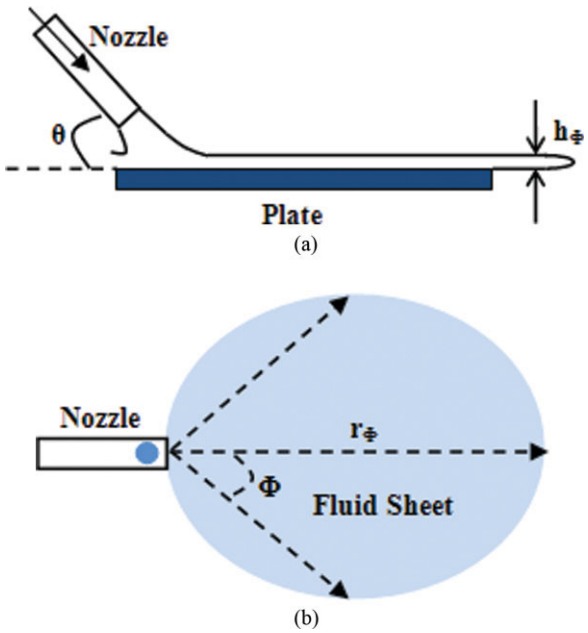

Figure 5. Schematic of the liquid sheet formation.

[Color figure can be viewed in the online issue, which is available at www.interscience.wiley.com.]

laminar boundary layer is expressed generally by the following equation using the cylindrical coordinate:

$$\left(\frac{d}{dr}+\frac{1}{r}\right)\int_0^{\delta} u(U_0-u)dz = v_1\left(\frac{\partial u}{\partial z}\right)_{z=0} \tag{1}$$

Equation 1 is solved using a polynomial velocity profile described by: $u_\phi = U_0[2\left(\frac{z}{\delta_\phi}\right)+2\left(\frac{z}{\delta_\phi}\right)^3+\left(\frac{z}{\delta_\phi}\right)^4]$. This equation is substituted in the momentum equation, the expression for boundary layer thickness is obtained as: $\delta^*_\phi = 5.97\sqrt{r^*_\phi}$. Then, the solution is divided into two parts based on whether the boundary layer is fully developed at the tip of the plate or not. The location of fully developed boundary layer is[3]

$$r^*_{\phi 0} = \frac{0.564}{(4\pi)^{1/3}}.A^{2/3}B^{4/3}, \tag{2}$$

where $r^*_{\phi 0}$ is non-dimensionalized as following.

$$A = \frac{\sin\theta}{\sin\phi^2+\cos\phi^2\sin\theta^2}, \tag{3}$$

$$B = -\cos\theta\left(\pm\sqrt{\frac{\sin\theta^2}{\tan\phi^2+\sin\theta^2}}\right)+\sqrt{1-\frac{\cos\theta^2\tan\phi^2}{\tan\phi^2+\sin\theta^2}} \tag{4}$$

$$r^*_{\phi 0} = \frac{r_{\phi 0}}{a}Re^{-\frac{1}{3}}, \tag{5}$$

and a is the jet radius, r_ϕ is the plate length and Re is Reynolds number defined as

$$\mathrm{Re} = \frac{\pi\rho_l a U_j}{\mu_l} \tag{6}$$

Now if $r_\phi \le r_{\phi 0}$, the relations for the sheet thickness and velocity distributions at the plate tip are[3]

$$h^*_\phi = \frac{1}{2r^*_\phi}A.B^2 + 1.79\sqrt{r^*_\phi} \tag{7}$$

$$U_{\phi,\mathrm{sh}} = U_j \tag{8}$$

where

$$h^*_\phi = \frac{h_\phi}{a}Re^{1/3} \tag{9}$$

and r^*_ϕ are non-dimensionalized in the same way as $r^*_{\phi 0}$.

If $r_\phi > r_{\phi 0}$, the relations for the sheet thickness and velocity distributions at the plate tip are[3]

$$h^*_\phi = \frac{0.642.A.B^2}{r^*_\phi}+\frac{5.03r^{*2}_\phi}{A.B^2}, \tag{10}$$

$$U_\phi = \frac{U_j}{0.8988+7.042.A^{-2}.B^{-4}.r^{*3}_\phi} \tag{11}$$

Lagrangian code

KIVA 3V-REL2 is chosen as the base code for the simulation. It uses Lagrangian droplet—Eulerian Fluid stochastic spray model. It considers a group of identical droplets known as a parcel, which is tracked in a Lagrangian framework whereas the gas phase is modeled using an Eulerian approach. The code consists of three parts: Pre-processor, Main-processor, and Post-processor. The pre-processor is sued for mesh generation, the processor is for spray simulations, and post-processor is employed for after simulation analysis. The code solves for three main equation of mass, momentum, and energy. It includes many different submodels such as turbulence, oscillation, and breakup (TAB model) and evaporation model (if necessary).

The splash plate model discussed earlier is implemented in the KIVA code as a submodel to simulate the whole spray dynamics. This submodel should determine the diameter, velocity, and number of droplets in the parcel based on the data from the splash plate model. In addition, the introduced sub model provides a new method for droplet breakup. In the original code, droplet breakup is modeled by changing the diameter, velocity, and number of droplets in a parcel, rather than physically breaking the parcel into two or more parcels. However, we have modeled the breakup process by breaking a parent parcel (injected from the nozzle) into several new parcels after the impingement on the plate.

Naber and Reitz[11] have used KIVA to study spray impingements on walls. Their spray model accounts for the effects of drop breakup, collision, and coalescence and the effect of drops on the gas turbulence. Three different drop-wall submodels were considered: stick, reflect, and jet. Trujillo and Lee[12] have conducted a numerical and analytical study of film formation and the evolution during spray

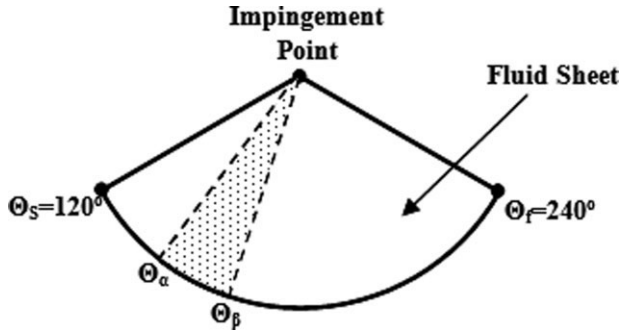

Figure 6. Slicing method to determine the number of droplets in each parcel.

impingement. Their model consists of two parts: impingement zone and spray zone. The impingement zone is modeled by using source terms based on conservation laws. In the spray zone, they have employed KIVA to simulate the spray.

The method which is used in this study is very similar to that of Naber and Reitz[11] and Trujillo and Lee[12] in its physical aspect but it is different in its application and implementation into numerical code. Their goal was to study spray (a discrete phase) interaction while our goal is to simulate jet impingement on the plate using its analogy with spray and discrete droplet impingement on the plate.

Parcel impinges on a plate and then breaks into smaller droplets moving along the plate. As explained, by definition in KIVA, breakup of a parcel means changing its characteristics (parcel diameter, velocity, and number of droplets in a parcel) from the initial parcel to the final parcel. Naber and Reitz[11] model is based on this definition and no physical breakup of a parcel into two or more parcels occurs. In our simulation, as the aim is to simulate jet impingement on a plate, it is necessary to break the impinged parcel into two or more parcels; as a result, some modifications are performed on KIVA and subroutines are added to make it capable of breaking a parcel after impingement into more parcels with different size, velocity, and number of droplets.

Two main equations used here are the momentum and mass conservation. Both equations have been applied once in the initial model presented by Inamura,[3] but the mass balance has to be applied once more to calculate the number of droplets in a parcel. When an injected parcel hits the splash plate, initially it has a specific mass with specific number of droplets. It breaks into several parcels in several directions. Each of these parcels has specific diameter and velocity. To conserve the mass, the following criteria should be justified

$$\dot{m}_{\text{initial}} = (4/3)\pi\rho_l N_{\text{ini}} r_{\text{p,ini}}^3 = (4/3)\pi\rho_l \sum_{i=0}^{n} N_i r_{\text{p},i}^3 \tag{12}$$

where N_{ini} is the number of droplets in the initial parcel (before impingement), $r_{\text{p,ini}}$ is radius of initial parcel, i is parcel number, n is number of produced parcels, N_i number of droplets in parcel i, $r_{\text{p},i}$ radius of parcel i. Now, the problem is finding N for each parcel while conserving the initial mass flux. To do so, fluid sheet has been descritized to many slices. Figure 6 shows the detail of our analysis.

To determine the number of droplets, the mass flux of each slice calculated at each of these sheet slices is represented by one final parcel. The mass flux through each slice is

$$\dot{m}_i = \rho_l r_\phi \int_{\theta_\alpha}^{\theta_\beta} h_i(\theta) V_i(\theta) d\theta \tag{13}$$

on the other hand, the initial mass flux may be reformulated as

$$\dot{m}_{\text{initial}} = \rho_l r_\phi \int_{\theta_s}^{\theta_f} h(\theta) V(\theta) d\theta \tag{14}$$

We define P_i as

$$P_i = \frac{\dot{m}_i}{\dot{m}_{\text{initial}}} = \frac{\int_{\theta_\alpha}^{\theta_\beta} h_i(\theta) V_i(\theta) d\theta}{\int_{\theta_s}^{\theta_f} h(\theta) V(\theta) d\theta}. \tag{15}$$

The mass of each final parcel in time is also equal to

$$m_i = N_i (4/3)\pi\rho r_{\text{p},i}^3. \tag{16}$$

From (15) and (16)

$$N_i \left(\frac{4}{3}\right)\pi\rho r_{\text{p},i}^3 = P_i m_{\text{initial}}, \tag{17}$$

and combining (17) with (12), we get

$$N_i \left(\frac{4}{3}\right)\pi\rho r_{\text{p},i}^3 = P_i (4/3)\pi\rho N_{\text{ini}} r_{\text{p,ini}}^3, \tag{18}$$

Therefore, N_i (the number of droplets produced when a parcel hits the plate) is

$$N_i = P_i N_{\text{ini}} \frac{r_{\text{initial}}^3}{r_{\text{p},i}^3} \tag{19}$$

Code setup

A simple geometry of nine cubical boxes is used as a chamber for the spray. One of them is specified for the

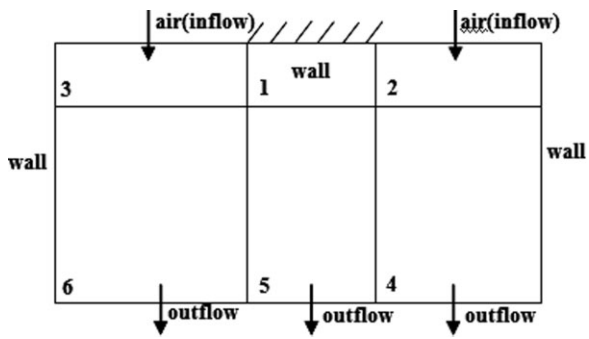

Figure 7. Solution domain.

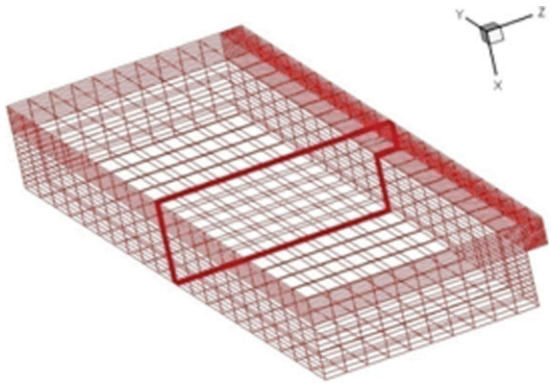

Figure 8. Mesh generated for the splash plate atomizer analysis.

[Color figure can be viewed in the online issue, which is available at www.interscience.wiley.com.]

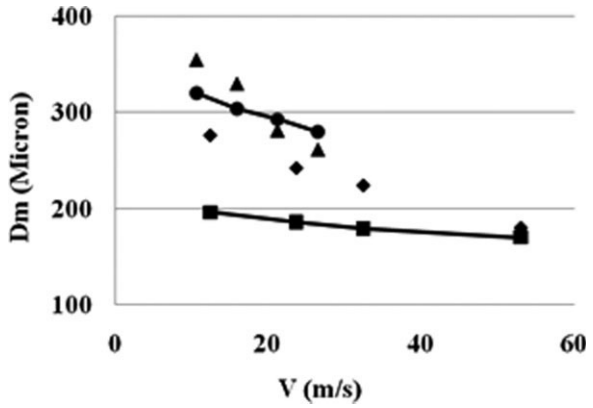

Figure 9. Measured and predicted mean droplet sizes generated from splash plate nozzle with nozzle diameters of 1 and 2 mm using water.

▲: $d_j = 2$ mm, experiment, ●: $d_j = 2$ mm, numerical, ◆: $d_j = 1$ mm, experiment, ■: $d_j = 1$ mm, numerical.

injection point and the splash plate. Figure 7 demonstrates the solution domain and its different regions. The mesh used for the simulations are shown in Figure 8. Domain size is 100*D* by 50*D* by 25*D*. The plate length varies depending on the nozzle, but in the majority of cases it is approximately 6*D*. The injection time is between 200 and 250 ms. This time is enough to reach the steady state conditions based on our investigations.

The simulation is performed for different cases to test the code accuracy. Although there are many experiments addressing jet impingement, but most of the studies do not provide sufficient input data for comparison with numerical results; for instance, the plate geometry specifications are not mentioned (e.g., plate length). Because of the mentioned problem, the code results are only compared with the experiments performed by Ahmed et al.[13] (small scale nozzle) and two other experiment for Spielbauer et al.[14] (large scale nozzle). The physical properties of experimental test are presented in Table 1. We have used exactly the same nozzle geometry as in the experiments.

Results

Figure 9 shows the comparison between the experimental results and the numerical data for nozzle diameters of 1 and 2 mm with water as running fluid. Four different velocities for each of the nozzles are tested. Both cases show a relatively good agreement with the experiments; although the 2 mm nozzle has better accuracy comparing with 1 mm nozzle. This may be due to the fact that the model for the sheet thickness distribution works better for thicker sheets because thin sheets may perforate early and not follow the sheet instability theory. Generally, we expect the mean size to decrease as velocity is increased. As the injection velocity is increased, liquid sheet spreads through a larger area resulting in a thinner sheet. Thinner sheets result in smaller droplet sizes at the center of the spray.

Two large scale nozzles, which are mentioned in Table 2 are also examined. The injection fluid is black liquor and the nozzle diameter is 9.5 mm, which is much larger than previously tested nozzles. Unfortunately, due to the lack of data it is not possible to compare more cases for large scale nozzles. Two injection velocities of 11 and 13.7 m/s are studied. The numerical results show good agreement with the experiments with a maximum error of 7%.

Table 1. Experimental Conditions Used to Examine the Numerical Results

Nozzle Diameter (mm)	Injection Velocity (m/s)	Injection Fluid
1.0	12.44	Water
1.0	23.7	Water
1.0	32.44	Water
1.0	53.03	Water
2.0	10.61	Water
2.0	15.92	Water
2.0	21.22	Water
2.0	26.63	Water
9.525	11	Black liquor
9.525	13.7	Black liquor

Spray droplet size and velocity

Figure 10 shows the droplet size distribution across the spray $50d_j$, downstream of the impingement point. Nozzle diameter is 2 mm, injection velocity is 21.2 m/s, and the running fluid is water. The size is maximum at the centerline with 320 μm and it decreases towards the edges. It reaches the minimum value of 140 μm and again it increases slightly to 180 μm. Droplet size at the center is expected to be the maximum since most of the mass flux flows through the center region and the sheet thickness is the maximum at the center region. Towards the edges of the spray, sheet thickness decreases, therefore, so does the droplet sizes. At the

Table 2. Comparison of the Numerical and Experimental Results for a Commercial Scale Splash Plate Nozzle with Black Liquor as Running Fluid

d_j (mm)	U_j (m/s)	d_m(Exp) (μm)	d_m(Num) (μm)	Err (%)
9.5	11	2810	2888	3
9.5	13.7	2470	2306	7

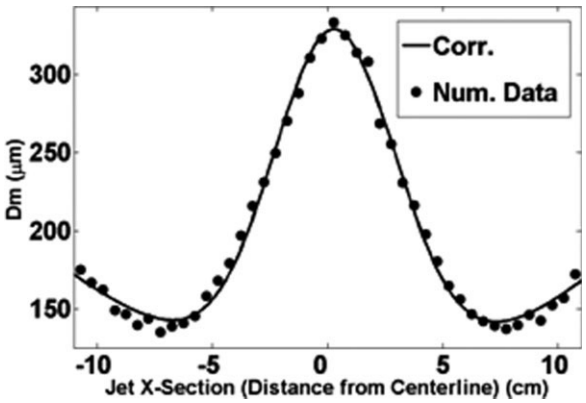

Figure 10. Droplet size distribution across the spray for the nozzle diameter of 2 mm and injection velocity of 21.2 m/s, the running fluid is water at room temperature.

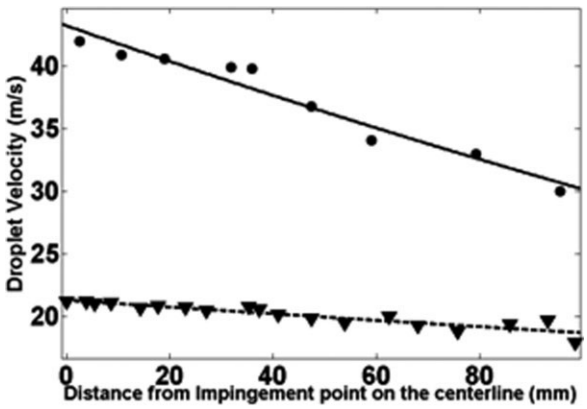

Figure 12. Velocity distribution along the spray centerline.

●: 1 mm, 42.2 m/s, ▼: 2 mm, 21.2 m/s.

extreme edges of the sheet, rim formation has been observed for most of the cases in the experiment. Neither the sheet formation model nor the simulation has accounted for the rim formation in its physical sense. But to compensate for the rim formation effect, the sheet thickness distribution from the wall model is assumed to be periodic accounting for the returning fluid from the backward flow in the sheet. This periodic function has compensated for the rim formation; therefore, we see a rise in the droplet size at the edges.

The droplet size distribution from the centerline to the edges declines by about 50%. This may be important in many applications, especially in combustion processes. In those processes, fuel mass distribution has direct effect on the fuel and oxidizer mixture and consequently on the combustion stoichiometry. Undesired stoichiometry can effect process efficiency, combustion temperature, and pollutant production.

The velocity distribution for the spray cross section at $50d_j$, downstream of the impingement point is shown in Figure 11. Two nozzle diameters of 1 and 2 mm with injection velocities of 42.2 and 21.2 m/s, respectively, and with water as running fluid are considered. The figure clearly shows that depending on the physical and operational conditions, the velocity distribution can take different profiles. For larger nozzles with larger droplets and lower velocities (due to the lower injection velocity), droplets with very low velocities (which will disperse randomly) in a location between the centerline and the extreme edge are observed. These low velocity droplets are observed in the case of 2 mm nozzle with low injection velocity and they cause the average velocity to be minimum somewhere between the centerline and spray edge. For the smaller nozzle of 1 mm with high injection velocity, no minimum velocity is observed.

The other important parameter to investigate is the spray velocity along the centerline from the impingement point onward. Figure 12 shows the spray velocity for the same two cases presented in Figure 11. It shows that in both cases the velocity decreases almost linearly with the distance from the impingement point. This decrease is more significant for the smaller nozzle, which has a higher jet velocity. Droplet velocities reduce by about 30% for the smaller nozzle, whereas the change for the larger nozzle is about 16%. The

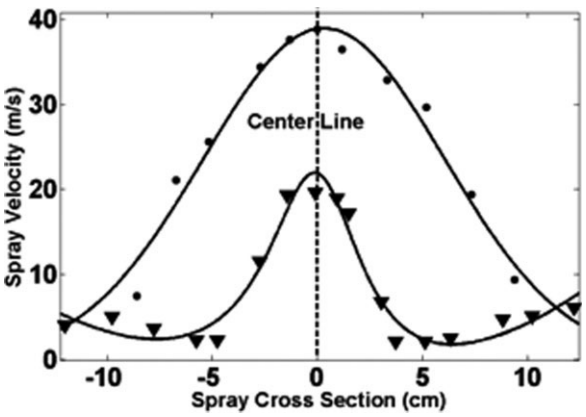

Figure 11. Velocity distribution at spray cross section downstream of the flow.

●: 1 mm, 42.2 m/s, ▼: 2 mm, 21.2 m/s.

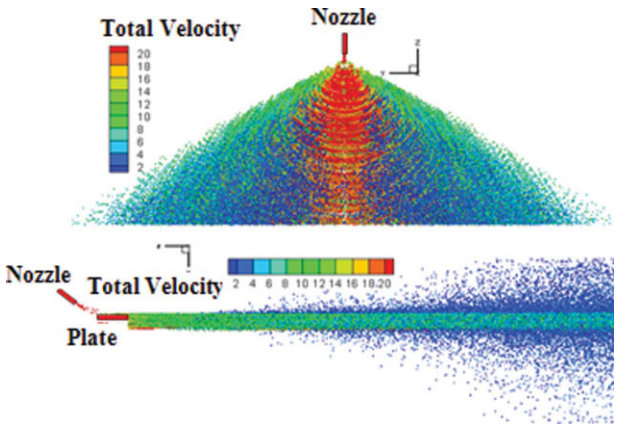

Figure 13. Velocity distribution of the spray for the nozzle diameter of 2 mm and injection velocity of 22 m/s, the running fluid is water at room temperature.

[Color figure can be viewed in the online issue, which is available at www.interscience.wiley.com.]

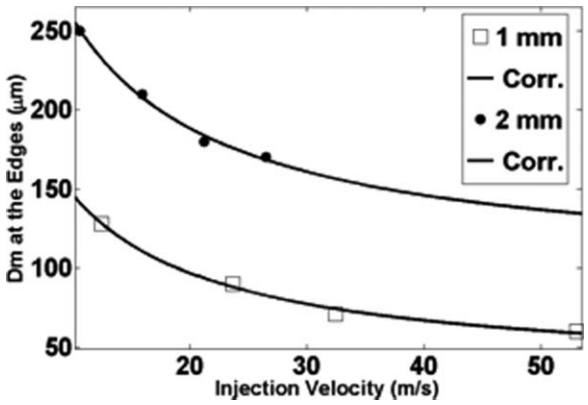

Figure 14. Droplet size distribution at the spray edges for different injection velocities.

smaller nozzle generates smaller droplets, which lose their momentum more rapidly than those for the larger droplets.

Figure 13 shows the top and the side views of the total velocity. The velocity is maximum on the centerline with 23–25 m/s and it decreases to 10–15 m/s at the edges. The flow slows down toward the downstream and reaches to 19–23 m/s on the centerline at the distance of $100d_j$ of the plate tip. The side view of the spray shows that the droplets are dispersing in the plane vertical to the spray sheet and they lose velocity (momentum) as they detach from the sheet in a random direction. The dispersion intensifies along the spray axis.

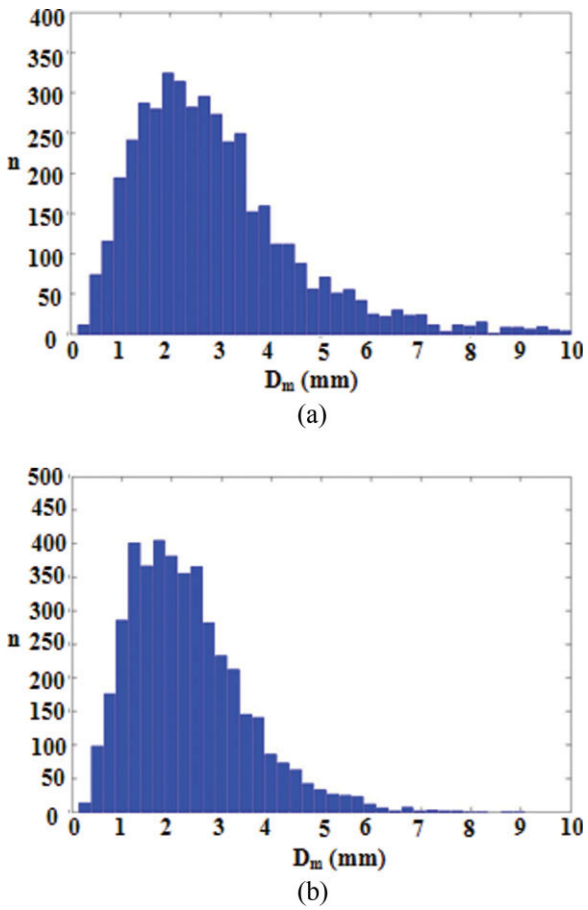

Figure 15. Droplet size distribution histogram at the center of the spray.

Nozzle diameter is 9.5 mm with black liquor as the fluid. (a) Injection velocity of 11 m/s and (b) injection velocity of 13.7 m/s. [Color figure can be viewed in the online issue, which is available at www.interscience.wiley.com.]

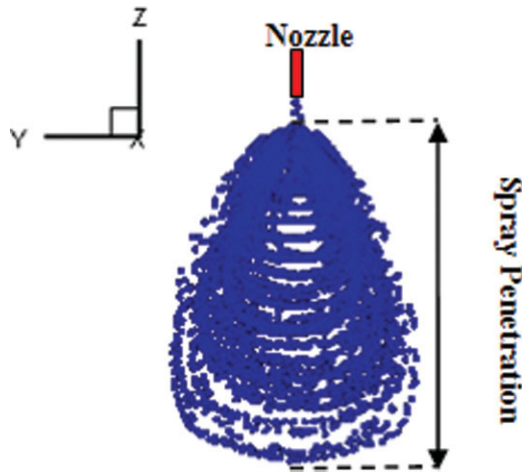

Figure 16. Spray tip penetration definition.

[Color figure can be viewed in the online issue, which is available at www.interscience.wiley.com.]

Figure 14 shows the average droplet sizes at the edge of the spray for the two cases discussed earlier. Comparing these results with those of Figure 9, which are for the same cases but on the spray centerline, a significant decrease in size from the center to edges is observed. The amount of decrease varies from 20% for 2 mm nozzle with injection velocity of 10.61 m/s to over 60% for 1 mm nozzle with the velocity of 53 m/s. For large nozzles with low injection velocity, rim formation is observed which will cause the droplet size to rise at the edges, decreasing the difference with the centerline. Small nozzles with high injection velocity (for a liquid sheet with no rim), the droplet size significantly decreases from the centerline to the edges.

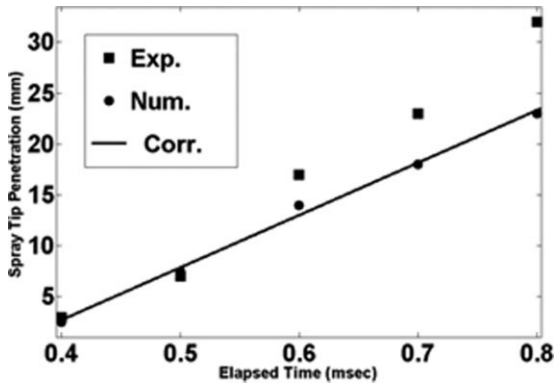

Figure 17. Time history of the spray tip penetration.

Figures 15a, b show the droplet size histogram at the center of the spray. The vertical axis is the number of parcels with the size specified on the horizontal axis. The majority of the droplet sizes are in the 1–4 mm range for the injection velocity of 11 m/s and 1–3 mm range for the injection velocity of 13.7 m/s. As the jet velocity is increased, the droplet distribution becomes narrower and more monosize droplets are produced.

Spray tip penetration

Spray tip penetration is also simulated and compared with an experimental result to validate the model in transient sprays. The transient spray starts with an initial injection and ends when the spray becomes fully developed. The time duration of the transient spray used is in the order of 1 ms. Figure 16 shows the definition of the spray tip penetration. Time evolution of spray tip is a measure of spray transient state which is the length from the plate edge to the tip of the spray. It is usually plotted vs. the elapsed time, which is the time passed from the injection start. Simulation is performed for an experiment reported by Inamura and Tomoda[15] with nozzle diameter of 0.33 mm and injection velocity of 50.5 m/s. The running fluid is a dry solvent with density of 775 kg/m^3, viscosity of 0.792 mPa S, and surface tension coefficient of 24.5 mN/m.

Figure 17 shows the numerical results for the tip penetration vs. elapsed time. The tip penetration is increasing almost linearly with time, which means that the spray is moving with almost constant velocity forward. Experimental data show a small acceleration in the spray tip, which is not observed in the model.

Summary and Conclusion

An atomization model for splash plate nozzles is developed, which replaces a continuous liquid sheet with discrete droplets. A KIVA-based model is used to model spray dynamics and droplet sizes further downstream of the nozzle. A theoretical wall model is used to determine the sheet thickness and velocity on the plate. The wall model includes the boundary layer development on the plate. The model comprises of the following steps:

- Sheet thickness and velocity distribution is determined on the plate in every angle according to the following relations:

$$\text{For } r_\phi \le r_{\phi 0} : h^*_\phi = \tfrac{1}{2r^*_\phi} A.B^2 + 1.79\sqrt{r^*_\phi} \quad \text{and} \quad U_{\phi,\text{sh}} = U_j$$

$$\text{For } r_\phi > r_{\phi 0} : h^*_\phi = \tfrac{0.642.A.B^2}{r^*_\phi} + \tfrac{5.03 r^{*2}_\phi}{A.B^2}$$

$$\text{and} \quad U_\phi = \frac{U_j}{0.8988 + 7.042.A^{-2}.B^{-4}.r^{*3}_\phi}$$

where all the parameters are defined throughout the text.

- Parcels of droplets, having a diameter and a velocity equal to those of local sheet thickness and velocity, are injected from the nozzle.
- Droplet parcels impinge on the plate.
- Number of droplets in a parcel after impingement are determined:

$$N_i = P_i N_{\text{ini}} \frac{r^3_{\text{initial}}}{r^3_{\text{p},i}}$$

where

$$P_i = \frac{\dot{m}_l}{\dot{m}_{\text{initial}}} \frac{\int_{\theta_\alpha}^{\theta_\beta} h_i(\theta) V_i(\theta) d\theta}{\int_{\theta_s}^{\theta_f} h(\theta) V(\theta) d\theta}$$

- Data from the above relations are associated to the newly produced parcels in every angle (*the new parcels are produced from the parent parcel which was impinged on the plate*).
- The newly produced parcels move along the plate and interact with the surrounding gas, and through collision and breakup.

Average droplet sizes predicted by the present model are in good agreement with those experiments under similar conditions.

The results show that the droplet sizes for splash plate nozzle are the largest at the centerline of the spray and the smallest between the centerline and the edges of the spray. Edge droplet size can be as low as half of the droplet size at the centerline of the spray.

The lowest droplet velocities may be between the edges and the centerline of the spray or at the edges of the spray. But generally, the lowest velocity for the droplets occur at the center of the spray and it decreases toward the edges.

Notation

Parameters

α = start angle in a slice of fluid sheet
β = end angle in a slice of fluid sheet
δ = boundary layer thickness
ρ = density
μ = viscosity
Φ = angle in the sheet plane
θ = nozzle angle
A, B = geometrical parameter
D = droplet diameter
N = number of droplets in a parcel
P = portion
Re = Reynolds number
U = velocity
a = nozzle radius
d = diameter
h = sheet thickness
$\dot{m}$ = mass flux
N = number of parcels
r_Φ = distance from impingement point to plate tip
r_p = parcel diameter

Subscripts

* = nondimensional
0 = fully developed boundary layer
Φ = parameter in the angle in the sheet plane
f = finish
g = gas
j = jet
i = parcel number i
ini = initial
l = liquid
m = mean
p = parcel
relative = relative velocity between gas and fluid
s = start
sh = sheet

Literature Cited

1. Ahmed M, Amighi A, Ashgriz N, Tran H. Characteristic of liquid sheet sprays formed by splash plate nozzles. *J Exp Fluids*. 2008;44:125–136.
2. Ahmed M, Amighi A, Ashgriz N, Tran H. Break-up length and spreading angle of liquid sheets formed by splash plate nozzles. *J Fluid Eng*. 2009;131, online article No. 011306.
3. Inamura T, Yanaoka H, Tomoda T. Prediction of mean droplet size of sprays issued from wall impingement injector. *AIAA J*. 2004;42: 614–621.
4. Taylor GI. Formation of thin flat sheets of water. *Proc R Soc Lond B Biol Sci*. 1960;259:1–17.
5. Dombrowski N, Hasson D, Ward DE. Some aspects of liquid through fan spray nozzles. *Chem Eng Sci*. 1960;12:35–50.
6. Savart F. Suite du memoire sur le choc d'une veine liquid lancee contre un plan circulaire. *Annl de Chimie et de Physique*. 1833;65: 54–113.
7. Dorman RG. The atomization of liquid in a flat spray. *Br J Appl Phys*. 1952;3:189–192.
8. Fraser RP, Eisenklam P. Research into the performance of atomizers of liquids. *Imp Colloid Chem Eng Soc J*. 1953;7:52–68.
9. Dombrowski N, Fraser RP. A photographic investigation into the disintegration of liquid sheets. *Trans R Soc London Ser A Math Phys Sci*. 1954;247.
10. Foust TD, Hamman KD, Detering BA. Numerical simulation of black liquor spray characteristics. *Proceedings of IMECE02*, New Orleans, 2002.
11. Naber JD, Reitz RD. Modeling engine spray/wall impingement. SAE Paper 880107.
12. Trujillo MF, Lee CFF. Modeling film dynamics in spray impingement. *Trans ASME*. 2003;125:104–112.
13. Ahmed M, Ashgriz N, Tran HN. Influence of breakup regime on the droplet sizes produced by splash-plate nozzles. *AIAA J*. In press.
14. Spielbauer TM, Adams TN, Monacelli JE, Bailey RT. Droplet size distribution of black liquor sprays. *IPC Tech Paper Seri*. 1989;325.
15. Inamura T, Tomoda T. Characteristics of sprays through a wall impingement injector. *J Atomization Sprays*. 2004;14:375–395.

Manuscript received Dec. 17, 2008, and revision received July 2, 2009.